HHS Public Access

Author manuscript

Biochem Biophys Res Commun. Author manuscript; available in PMC 2022 May 14.

Published in final edited form as:

Biochem Biophys Res Commun. 2021 May 14; 553: 180–186. doi:10.1016/j.bbrc.2021.03.047.

Bok binds to a largely disordered loop in the coupling domain of type 1 inositol 1,4,5-trisphosphate receptor

Laura M. Szczesniak[1], **Caden G. Bonzerato**[1], **Jacqualyn J. Schulman**[1], **Alaji Bah**[2], **Richard J. H. Wojcikiewicz**[1,*]

[1]Department of Pharmacology, SUNY Upstate Medical University, Syracuse, NY, USA.

[2]Department of Biochemistry and Molecular Biology, SUNY Upstate Medical University, Syracuse, NY, USA.

Abstract

Bcl-2-related ovarian killer (Bok) binds tightly to inositol 1,4,5-trisphosphate receptors (IP_3RS). To better understand this interaction, we sought to elucidate the Bok binding determinants in IP_3R1, focusing on the ~ 75 amino acid loop (residues 1882-1957) between α helices 72 and 73. Bioinformatic analysis revealed that the majority of this loop is intrinsically disordered, with two flanking regions of high disorder next to a low disorder central region (~residues 1914-1926) that is predicted to contain two fused, disjointed transient helical elements. Experiments with IP_3R1 mutants, combined with computational analysis, indicated that small deletions in this central region block Bok binding due to perturbation of the helical elements. Studies *in vitro* with purified Bok and IP_3R1-derived peptides revealed high affinity binding to amino acids 1898-1940 of IP_3R1 (K_d ~65nM) and that binding affinity is also dependent upon both of the high disorder flanking regions. The strength of the Bok-IP_3R1 interaction was demonstrated by the ability of IP_3R1 or Bok to recruit transmembrane domain-free Bok or IP_3R1 mutants, respectively, to membranes in intact cells, and that these two mutants can bind in the cytosol independently of membrane association. Overall, we show that Bok binding to IP_3R1 occurs within a largely disordered loop between α helices 72 and 73 and that high affinity binding is mediated by multivalent interactions.

Keywords

Bcl-2 related ovarian killer (Bok); inositol 1,4,5-trisphosphate receptor; calcium; intrinsically disordered region; secondary structure; protein-protein interaction

*Corresponding author. Department of Pharmacology, SUNY Upstate Medical University, 750 E. Adams Street, Syracuse, NY 13210. 315-464-7956 wojcikir@upstate.edu.

The authors declare no conflict of interest.

1. Introduction

Bcl-2-related ovarian killer (Bok) is a poorly-characterized protein in the Bcl-2 family, with several studies in recent years indicating that Bok can play pro-, anti-, or non-apoptotic roles [1, 2]. Bok contains 213 amino acids and is anchored to membranes by its C-terminal transmembrane (TM) domain [1, 2].

Despite the confusion that surrounds the role of Bok, one certainty is its interaction with inositol 1,4,5-trisphosphate receptors (IP_3Rs) [3-5], which are tetrameric Ca^{2+} channels found in the endoplasmic reticulum (ER) membrane of mammalian cells [6]. The nature of Bok binding to IP_3Rs is unique compared to other Bcl-2 family proteins [7], as it appears that essentially all cellular Bok is constitutively bound to IP_3Rs [3, 4]. Further, in the absence of IP_3Rs, Bok is rapidly degraded by the proteasome [4]. Previous studies have demonstrated that Bok binds to IP_3R1 via its helical BH4 domain, and that point mutations that distort the BH4 helix completely abrogate binding [3]. Thus far, information on the location of the Bok binding site on IP_3Rs has only come from IP_3R1 truncation mutations [3], and suggests that Bok binds within the coupling domain of IP_3R1, and perhaps to a loop between α helices 72 and 73 (α72-73 loop) [3, 8].

Here, using mutagenesis of full-length IP_3R1, *in vitro* studies with purified proteins and computational analysis, we show that the Bok binding determinants in IP_3R1 are exclusively located in the α72-73 loop, the majority of which is intrinsically disordered, that IP_3R1s with very small deletions do not bind Bok, and that high affinity binding is mediated by multiple determinants within the α72-73 loop.

2. Materials and methods

2.1 Materials

HEK-3KO cells were created and maintained as described [9]. Rabbit antibodies were: anti-HA [3] (used for IP), anti-$IP_3R1^{1884\text{-}1903}$ (Enzo), anti-Hrd1 [10], anti-transaldolase [10], and anti-Bok [3]. Mouse monoclonal antibodies were: anti-HA (Berkeley Antibody Co. for immunoblot) and anti-p97 (Research Diagnostics Inc.). PCR reagents were from New England BioLabs. SDS-PAGE reagents were from BioRad. Protein A-Sepharose CL-4B was from GE Healthcare. Linear, MW~25,000 polyethylenimine (PEI) was from Polysciences Inc. Horseradish peroxidase-conjugated secondary antibodies, protease inhibitors, and all other reagents not listed were from Sigma.

2.2 Mutagenesis

All IP_3R1 mutants were created from mouse IP_3R1 tagged at the C-terminus with an HA epitope (IP_3R1-HA) [3] by inverse PCR, with insertion of either a NheI or XhoI site, to facilitate screening. $IP_3R1\text{-}HA^{\Delta TM}$ contains amino acids 1-2264 of IP_3R1. Bok from mouse tagged at the N-terminus with a 3xFlag epitope (3F-Bok) [3] was used to create $3F\text{-}Bok^{\Delta TM}$, which contains amino acids 1-187 of Bok, by inverse PCR, with insertion of a BamHI site. Primer sequences are available upon request. The authenticity of all cDNAs was confirmed by DNA sequencing (Genewiz).

2.3 Analysis of Bok/IP$_3$Rs and cellular fractionation

HEK-3KO cells were seeded in 6-well plates (Corning) at 6-8x10^5/well and transfected ~24 h later with 1-2 μg cDNAs and 6μL of 1mg/mL PEI. Cell lysates were prepared for IP as described [3]. To obtain crude membrane and cytosol fractions, cells were harvested with ice-cold homogenization buffer and sonicated [10], were centrifuged at 20,000*xg* for 60 min at 4°C, supernatants were collected, and pellets were resuspended in homogenization buffer. All samples were resuspended in gel-loading buffer, incubated at 37°C for 30 min or boiled for 5 min, subjected to SDS-PAGE, and proteins were transferred to nitrocellulose for probing as described [4]. Immunoreactivity was detected using Pierce ECL reagents and a Chemidoc (Bio-Rad). Mass markers (in kDa) are indicated on the right side of all immunoblots.

2.4 Protein purification, fluorescence polarization (FP), and in vitro assays

FITC-conjugated peptides and mouse Bok/IP$_3$R1 DNA sequences were from GenScript. Sequences were subcloned from the pUC57 vector into a pET SUMO vector (Invitrogen), which contains a His-sumo (HS) tag, using Gibson assembly (primers available upon request). Proteins were expressed in BL21-CodonPlus (DE3)-RIPL E. coli cells (Agilent Technologies) in Luria broth containing kanamycin and chloramphenicol, and cultured at 37°C until OD_{600}~0.6. After incubation with 1 mM IPTG for ~18h at 16°C, pelleted cells were re-suspended in phosphate buffer (300 mM NaCl, 50 mM Na_2HPO_4/NaH_2PO_4, 20 mM imidazole, 1 mM benzamidine, 5 mM beta-mercaptoethanol, 100 mM arginine-HCl, pH 7.4, 100 mM glutamine, 5% glycerol) supplemented with lysozyme, were sonicated for 5 minutes, and were centrifuged at 27,000*xg* for 30 min at 4°C. HS-tagged proteins were purified using a nickel-nitriloacetic acid column (GoldBio), and eluted using the same phosphate buffer enriched with imidazole (400 mM). FP [11] was performed in PBS (pH 7.4) / 0.1% BSA using a Flex Station 3 (excitation 485 nm / emission 525 nm). Traces shown are the average of duplicate values for an individual representative experiment. K_d values were determined using GraphPad Prism after subtraction of non-specific signal (nonlinear regression, Binding-Saturation, one site – specific binding).

3. Results

3.1 Determinants of Bok-IP$_3$R1 binding

Previous studies with IP$_3$R1 N-terminal truncation mutants have suggested that the Bok binding site on IP$_3$R1 lies within the α72-73 loop [3], which contains well-characterized sites for caspase-3 and chymotrypsin cleavage, as well as many of the sites at which IP$_3$R1 is ubiquitinated (Fig. 1A) [12]. This approach is far from ideal, however, because the truncated IP$_3$Rs will certainly be structurally compromised and will have functional deficits. Therefore, we sought to create a “full-length” mutant of IP$_3$R1 that does not bind Bok. Several deletions were created in IP$_3$R1-HA within the α72-73 loop (Fig. 1A) and constructs were assessed for interaction with 3F-Bok^{WT} by immunoprecipitation (IP) from HEK cells lacking all endogenous IP$_3$Rs (HEK-3KO cells, Fig. 1B) [9]. IP of IP$_3$R1-HA^{WT} allowed for efficient co-IP of 3F-Bok^{WT} (Fig. 1B, lane 2), while the construct with the largest deletion, IP$_3$R1-HA$^{\Delta 1909\text{-}1941}$ did not co-IP 3F-Bok^{WT} (lane 3). Remarkably, constructs with much smaller deletions, IP$_3$R1-HA$^{\Delta 1916\text{-}1917}$, IP$_3$R1-HA$^{\Delta 1917}$ and IP$_3$R1-HA$^{\Delta 1920\text{-}1921}$ (lanes

4-6), all also failed to co-IP 3F-Bok^{WT}, demonstrating that the integrity of this region, rather than a discrete amino acid sequence, is important for IP$_3$R1-Bok binding. Interestingly, substitution of amino acids 1916-1917 with two adjacent glycine residues, which has been shown previously to break any potential α helices or structural motifs [4, 13], did not inhibit 3F-Bok^{WT} co-IP (lane 7). All mutants examined exhibited normal Ca^{2+} channel function, indicating that inability to bind Bok is not due to major structural perturbation outside of the ~1920 region (Supplementary Data, Fig 1).

The α72-73 loop is part of a small percentage of the IP$_3$R1 sequence that could not be resolved by cryo-EM [8, 14], suggesting it might be an intrinsically disordered region (IDR) [15]. IUPred2A disorder analysis [16] revealed that the majority of the α72-73 loop is indeed intrinsically disordered, with two regions of high disorder flanking a low disorder central region (~residues 1914-1926; Fig 1C). This “dip” in IUPred2 score and corresponding “peak” in ANCHOR2 score, an index of binding propensity, coincides perfectly with the region shown to be critical for Bok binding in co-IP experiments (Fig. 1B). Overall, these data indicate that the α72-73 loop is largely an IDR and that the central region of this loop is critical for Bok binding.

Secondary structure prediction of the loop identified regions with helical propensity, but did not reach a consensus on their positions (Supplementary Data, Fig. 2). Further analysis using Agadir, a program that predicts helical propensity based on the helix/coil transition theory [17], revealed clear helical propensity in the central region and, specifically, two discrete, but fused α-helical motifs (Fig. 1D). The first motif has low helical propensity (~5%) and spans residues E^{1908}-S^{1919}, while the second motif has relatively high helical propensity (~17%) and spans residues A^{1920}-A^{1925}. Interestingly, the two helices are non-contiguous, with each having its own register. Helical prediction for the IP$_3$R1 mutations that abrogate binding reveal that they either stabilize the first helix (Fig. 1E, F) or destabilize the second helix (Fig. 1G). Substitution of amino acids 1916 and 1917 with glycine, which did not block Bok binding, resulted in a significant destabilization of the first helix (Fig. 1H). Taken together, these results demonstrate that Bok binding is dependent on a relatively low and high helical propensity for the first and second motifs, respectively.

3.2 In vitro binding studies using purified Bok and IP$_3$R1 peptides

To further resolve the Bok binding site in IP$_3$R1, we sought to recapitulate the Bok-IP$_3$R1 interaction *in vitro* using bacterially expressed, HS-tagged proteins (Fig. 2A). Examination of protein purity (Fig. 2B), revealed major bands for HS-Bok and HS-IP$_3$R1 at the expected sizes of 36 and 25.5 kDa, respectively, with minor contaminants, likely corresponding to N-terminal fragments of HS-Bok and HS-IP$_3$R1. The interaction of HS-Bok and HS-IP$_3$R1 was shown via IP of IP HS-IP$_3$R1 (Fig. 2C); strong co-IP of the major band of HS-Bok was seen at 36 kDa, but not the HS-Bok fragment (lane 6), and no co-IP was seen with HS-HA (lane 7), which serves to demonstrate specificity.

We also analyzed the binding of FITC-tagged peptides corresponding to regions of the α72-73 loop (Fig. 2D) using a FP assay [11]. HS-Bok (Fig. 2B, lane 5), but not negative control HS-HA (lane 4), bound with high affinity to FITC-IP$_3$R1$^{1898-1940}$, which encompasses a large portion of the IP$_3$R1 α72-73 loop (Fig. 3E, K_d=64 ± 8 nM).

Remarkably, deleting the amino acids corresponding to positions 1916-1917 within this peptide completely blocked the binding (Fig. 2E), similarly to the properties of the IP_3R1-$HA^{\Delta 1916\text{-}1917}$ mutant described in Figure 1, indicating that these *in vitro* experiments accurately recapitulate events seen in intact cells.

Additional peptides were examined (Fig. 2D), including a shorter peptide, FITC-$IP_3R1^{1907\text{-}1921}$, which encompasses just the ANCHOR2 "peak" shown in Figure 1C, as well as FITC-$IP_3R1^{1898\text{-}1929}$ and FITC-$IP_3R1^{1904\text{-}1940}$, which lack portions of the C-terminal or N-terminal highly disordered flanking regions, respectively (Fig. 1A, C). We found that both $IP_3R1^{1898\text{-}1929}$ and FITC-$IP_3R1^{1904\text{-}1940}$ bound to HS-Bok, but with lower affinity than FITC-$IP_3R1^{1898\text{-}1940}$, as indicated by higher K_d values (265 ± 135 and 398 ± 126 nM, respectively), and that FITC-$IP_3R1^{1907\text{-}1921}$ does not bind to HS-Bok at all (Fig. 2F). Agadir analysis (Fig. 2G-J) appears to explain the inability of FITC-$IP_3R1^{\Delta 1916\text{-}1917}$ and FITC-$IP_3R1^{1907\text{-}1921}$ to bind, since the former peptide exhibits an increase in stability in the first α-helical motif (Fig. 2G) and the latter peptide completely lacks the second motif (Fig. 2H). Interestingly, the peptides lacking portions of the flanking disordered regions, that bind Bok with lower affinity, maintained a helical pattern similar to FITC-$IP_3R1^{1898\text{-}1940}$ (Fig. 2I, J). Taken together, these data indicate that high affinity binding of Bok to the α72-73 loop of IP_3R1 is dependent upon more than just the helical integrity of the central region of the loop; it also requires the presence of both of the highly disordered flanking regions.

3.3 Analysis of the Bok-IP_3R1 interface

While Bok binds IP_3Rs via its BH4 helix [3, 4], the structure of Bok [18] indicates that this helix is not fully exposed, as an unstructured loop lies across it (Fig. 3A, B). This occlusion likely prevents the BH4 helix from forming a long "helix to helix" interaction with the central helical region of the α72-73 loop. However, the BH4 helix surface that is critical for IP_3R binding is positively charged (Fig. 3C), prompting us to examine whether the IP_3R1 α72-73 loop might also be charged. Analysis using the CIDER program [19] revealed that the α72-73 loop contains a pattern of alternating charge blocks and that the central region of the loop, that is critical for Bok binding, contains a negatively charged area (Fig. 3D), suggesting that electrostatic interactions contribute to binding.

3.4 Bok and IP_3Rs associate independently of membrane insertion

Bok is constitutively associated with IP_3Rs [3], but it is unclear at what point in protein maturation the Bok-IP_3R1 interaction begins and whether this interaction is needed for normal ER membrane insertion. Interestingly, exogenous IP_3R1-HA^{WT} and exogenous 3F-Bok^{WT} localize completely to membranes when expressed alone (Fig. 4A, lanes 4 and 6, respectively), and when both IP_3R1-HA^{WT} and 3F-Bok^{WT} are co-expressed, the same localization is maintained, with an increase in Bok expression level (lane 8) [4]. Therefore, both Bok and IP_3Rs are able to independently "self-recruit" to membranes.

To explore when Bok and IP_3R1 interact, a Bok construct lacking the C-terminal TM domain (3F-$Bok^{\Delta TM}$) was examined. 3F-$Bok^{\Delta TM}$ is predominantly cytosolic (Fig. 4B, lane 1), but becomes membrane-associated and expression is increased upon co-transfection with IP_3R1-HA^{WT} (lanes 3-4), an effect not seen with the Bok binding-deficient mutant IP_3R1-

HA$^{\Delta 1916\text{-}1917}$ (lanes 5-6). Thus, the Bok-IP$_3$R1 interaction can occur prior to Bok membrane insertion and is strong enough to retain 3F-Bok $^{\Delta TM}$ in the membrane fraction.

Remarkably, a similar conclusion can be drawn from examination of an IP$_3$R1 construct lacking all 6 C-terminal TM domains (IP$_3$R1-HA$^{\Delta TM}$). When expressed in the absence of Bok, IP$_3$R1-HA$^{\Delta TM}$ is predominantly cytosolic (Fig 4C, lanes 1-2), but becomes more membrane-associated upon co-transfection of 3F-Bok^{WT} (lanes 3-4), an effect not seen with IP$_3$R1-HA$^{\Delta TM,\ \Delta 1916\text{-}1917}$, which lacks TM domains and the ability to bind Bok (lanes 5- 6).

Thus, the Bok-IP$_3$R1 interaction is robust enough for IP$_3$R1-HA^{WT} and 3F-Bok^{WT} to localize TM domain-lacking Bok and IP$_3$R1 constructs, respectively, to membranes, and that the interaction between Bok and IP$_3$R1 can occur independently of membrane insertion. This was confirmed by the observation that 3F-Bok and IP$_3$R1-HA co-IP regardless of TM status (Fig. 4D), and more importantly, that cytosolic 3F-Bok$^{\Delta TM}$ and IP$_3$R1-HA$^{\Delta TM}$ strongly co-IP (lane 6).

4. Discussion

Since its discovery, the cellular role of Bok has remained elusive and confusing [1, 2]. Some of this may stem from efforts to assign Bok a role within the intrinsic apoptosis pathway, and indeed, many now consider that Bok plays a conventional Bak/Bax-type pro-apoptotic role at the outer mitochondrial membrane [1, 2, 20]. Bok, however, is unlike other Bcl-2 family members, largely for the fact that it is uniquely and constitutively bound to ER-localized IP$_3$Rs [3,4].

Here we provide insight into the Bok-IP$_3$R1 interaction and have narrowed down the Bok binding site on IP$_3$R1 to a small region between α helices 72 and 73. The recent cryo-EM models of IP$_3$R1 [8, 14] have provided a wealth of information regarding the overall structure of the channel, but unfortunately did not resolve the α72-73 loop. Our data indicates that this is because the α72-73 loop is an IDR, composed of two highly disordered regions flanking a low disorder region in the central part of the loop that coincides with an increase in ANCHOR2 score, and is precisely the region in which small deletions in full-length IP$_3$R1 block Bok binding. Interestingly, perturbation of the highly disordered flanking regions decreased the affinity of the Bok-IP$_3$R1 interaction, suggesting that these regions also play a role in Bok binding. This is consistent with our previous findings in intact cells that an IP$_3$R1 mutant lacking amino acids 1-1903 does not bind Bok [3]; this mutant lacks part of the N-terminal highly disordered region. Overall, these data demonstrate that the Bok-IP$_3$R1 interaction requires both the central, low disorder region of the α72-73 loop, along with the highly disordered flanking regions for maximum binding affinity.

Agadir analysis revealed that the central region of the loop is composed of two contiguous α-helical motifs in different registers, and that the first helix may have to be relatively unstable in order for the second helix to participate in binding. Further, helical propensity did not change significantly upon removal of the N-terminal or C-terminal disordered regions, indicating that the disordered flanking regions and the more ordered central region of the loop can independently contribute to binding affinity. Thus, there appear to be four

determinants for the α72-73 loop interaction with Bok: (i) a disordered N-terminal flanking region, followed by (ii) a region with low helical propensity (E^{1909}-S^{1919}) that is fused to (iii) a region with high helical propensity (A^{1920}-A^{1925}), and finally (iv) a disordered C-terminal flanking region. Given the charge distributions in Bok and the α72-73 loop, it is likely that electrostatic interactions, together with the disjointed nature of the helical motifs within the α72-73 loop, mediate the strong interactions between IP_3R1 and Bok.

As well as binding Bok, the α72-73 loop contains sites for several post-translational modifications (PTMs) (Fig. 1A) [6, 12], consistent with findings for other IDRs [21]. Bok binding has been shown to protect IP_3R1 from proteolytic cleavage within the α72-73 loop [3], apparently due to steric hindrance, and may regulate other PTMs. While binding to IP_3Rs is critical for Bok stability [4], it does not appear to regulate Ca^{2+} channel function (Supplementary Data, Fig. 1) [5], and other potential roles for the interaction (e.g. in controlling mitochondrial morphology [5]) are currently being investigated. With regard to a possible role in membrane insertion, it is remarkable that the Bok-IP_3R1 interaction is strong enough to allow for both Bok and IP_3R1 to recruit to membranes TM domain-lacking versions of their counterparts, and for TM domain-lacking versions of each protein to co-IP. Thus, the Bok-IP_3R1 interaction can occur in the cytosol prior to membrane insertion. These studies also reveal that that the stabilization of Bok that results from binding to IP_3R1 [4] can occur independently of membranes, suggesting that the pathway that mediates Bok degradation may be cytosol-based, rather than ER-based, which has been previously suggested [4, 20].

In addition to Bok, several other Bcl-2 family proteins have been reported to interact with IP_3Rs, including Bcl-2 and Bcl-x_L [7]. Both of these proteins can interact with IP_3R1 via their BH4 domains [7], similarly to Bok [3]. However, they interact with IP_3R1 at a site different from the α72-73 loop and much less strongly than Bok [3]. Interestingly, the Bcl-2-IP_3R1 interaction has been extensively studied [22], leading to the creation of a small peptide inhibitor, BIRD-2, that is a potential therapeutic agent [22, 23]. It seems likely that the information obtained in the present study will guide future work that seeks to interfere with the Bok-IP_3R1 interaction and may lead to useful inhibitory compounds.

Supplementary Material

Refer to Web version on PubMed Central for supplementary material.

Acknowledgements

The authors thank Drs. Kamil Alzayady and David Yule, University of Rochester, for providing HEK-3KO cells, Dr. Thomas Kaufmann, University of Bern, Switzerland, for providing anti-Bok and Bok^{WT} cDNA, Dr. Andras Perl for providing anti-TAL, Dr. Stewart Loh and Xiaokong Gao for help with FP experiments, Fanghui Hua for providing HS-HA, and Katherine Keller for technical assistance. This work was supported by the National Institutes of Health Grants DK107944, GM121621 and GM134638.

Abbreviations:

Bok	Bcl-2-related ovarian killer
ER	endoplasmic reticulum

FP	fluorescence polarization
IDR	intrinsically disordered region
IP_3R	inositol 1,4,5-trisphosphate receptor
PTM	post-translational modification
TM	transmembrane

References

[1]. Naim S, Kaufmann T, The Multifaceted Roles of the BCL-2 Family Member BOK, Front Cell Dev Biol 8 (2020) 574338. [PubMed: 33043006]

[2]. Shalaby R, Flores-Romero H, Garcia-Saez AJ, The Mysteries around the BCL-2 Family Member BOK, Biomolecules 10(12) (2020).

[3]. Schulman JJ, Wright FA, Kaufmann T, Wojcikiewicz RJ, The Bcl-2 protein family member Bok binds to the coupling domain of inositol 1,4,5-trisphosphate receptors and protects them from proteolytic cleavage, J Biol Chem 288(35) (2013) 25340–9. [PubMed: 23884412]

[4]. Schulman JJ, Wright FA, Han X, Zluhan EJ, Szczesniak LM, Wojcikiewicz RJ, The Stability and Expression Level of Bok Are Governed by Binding to Inositol 1,4,5-Trisphosphate Receptors, J Biol Chem 291(22) (2016) 11820–8. [PubMed: 27053113]

[5]. Schulman JJ, Szczesniak LM, Bunker EN, Nelson HA, Roe MW, Wagner LE 2nd, Yule DI, Wojcikiewicz RJH, Bok regulates mitochondrial fusion and morphology, Cell Death Differ 26(12) (2019) 2682–2694. [PubMed: 30976095]

[6]. Prole DL, Taylor CW, Structure and Function of IP3 Receptors, Cold Spring Harb Perspect Biol 11(4) (2019).

[7]. Ivanova H, Vervliet T, Monaco G, Terry LE, Rosa N, Baker MR, Parys JB, Serysheva II, Yule DI, Bultynck G, Bcl-2-Protein Family as Modulators of IP3 Receptors and Other Organellar Ca(2+) Channels, Cold Spring Harb Perspect Biol 12(4) (2020).

[8]. Fan G, Baker ML, Wang Z, Baker MR, Sinyagovskiy PA, Chiu W, Ludtke SJ, Serysheva II, Gating machinery of InsP3R channels revealed by electron cryomicroscopy, Nature 527(7578) (2015) 336–41. [PubMed: 26458101]

[9]. Alzayady KJ, Wang L, Chandrasekhar R, Wagner LE 2nd, Van Petegem F, Yule DI, Defining the stoichiometry of inositol 1,4,5-trisphosphate binding required to initiate Ca2+ release, Sci Signal 9(422) (2016) ra35. [PubMed: 27048566]

[10]. Pearce MM, Wang Y, Kelley GG, Wojcikiewicz RJ, SPFH2 mediates the endoplasmic reticulum-associated degradation of inositol 1,4,5-trisphosphate receptors and other substrates in mammalian cells, J Biol Chem 282(28) (2007) 20104–15. [PubMed: 17502376]

[11]. Moerke NJ, Fluorescence Polarization (FP) Assays for Monitoring Peptide-Protein or Nucleic Acid-Protein Binding, Curr Protoc Chem Biol 1(1) (2009) 1–15. [PubMed: 23839960]

[12]. Wojcikiewicz RJH, Inositol 1,4,5-trisphosphate receptor degradation pathways, Wiley Interdisciplinary Reviews: Membrane Transport and Signaling 1(2) (2012) 126–135.

[13]. Monaco G, Decrock E, Nuyts K, Wagner LE 2nd, Luyten T, Strelkov SV, Missiaen L, De Borggraeve WM, Leybaert L, Yule DI, De Smedt H, Parys JB, Bultynck G, Alpha-helical destabilization of the Bcl-2-BH4-domain peptide abolishes its ability to inhibit the IP3 receptor, PLoS One 8(8) (2013) e73386. [PubMed: 24137498]

[14]. Fan G, Baker MR, Wang Z, Seryshev AB, Ludtke SJ, Baker ML, Serysheva II, Cryo-EM reveals ligand induced allostery underlying InsP3R channel gating, Cell Res 28(12) (2018) 1158–1170. [PubMed: 30470765]

[15]. Hong S, Choi S, Kim R, Koh J, Mechanisms of Macromolecular Interactions Mediated by Protein Intrinsic Disorder, Mol Cells 43(11) (2020) 899–908. [PubMed: 33243935]

[16]. Erdos G, Dosztanyi Z, Analyzing Protein Disorder with IUPred2A, Curr Protoc Bioinformatics 70(1) (2020) e99. [PubMed: 32237272]

[17]. Munoz V, Serrano L, Elucidating the folding problem of helical peptides using empirical parameters, Nat Struct Biol 1(6) (1994) 399–409. [PubMed: 7664054]

[18]. Zheng JH, Grace CR, Guibao CD, McNamara DE, Llambi F, Wang YM, Chen T, Moldoveanu T, Intrinsic Instability of BOK Enables Membrane Permeabilization in Apoptosis, Cell Rep 23(7) (2018) 2083–2094 e6. [PubMed: 29768206]

[19]. Holehouse AS, Das RK, Ahad JN, Richardson MO, Pappu RV, CIDER: Resources to Analyze Sequence-Ensemble Relationships of Intrinsically Disordered Proteins, Biophys J 112(1) (2017) 16–21. [PubMed: 28076807]

[20]. Llambi F, Wang YM, Victor B, Yang M, Schneider DM, Gingras S, Parsons MJ, Zheng JH, Brown SA, Pelletier S, Moldoveanu T, Chen T, Green DR, BOK Is a Non-canonical BCL-2 Family Effector of Apoptosis Regulated by ER-Associated Degradation, Cell 165(2) (2016) 421–33. [PubMed: 26949185]

[21]. Owen I, Shewmaker F, The Role of Post-Translational Modifications in the Phase Transitions of Intrinsically Disordered Proteins, Int J Mol Sci 20(21) (2019).

[22]. Distelhorst CW, Targeting Bcl-2-IP3 receptor interaction to treat cancer: A novel approach inspired by nearly a century treating cancer with adrenal corticosteroid hormones, Biochim Biophys Acta Mol Cell Res 1865(11 Pt B) (2018) 1795–1804. [PubMed: 30053503]

[23]. Kerkhofs M, La Rovere R, Welkenhuysen K, Janssens A, Vandenberghe P, Madesh M, Parys JB, Bultynck G, BIRD-2, a BH4-domain-targeting peptide of Bcl-2, provokes Bax/Bak-independent cell death in B-cell cancers through mitochondrial Ca(2+)-dependent mPTP opening, Cell Calcium 94 (2021) 102333. [PubMed: 33450506]

- The Bcl-2 protein family member Bok binds strongly to IP_3R1
- The binding site in IP_3R1 is a largely disordered loop in the coupling domain
- Multiple loop determinants including helical regions mediate high affinity binding
- The Bok-IP_3R1 interface represents a novel target for drug development

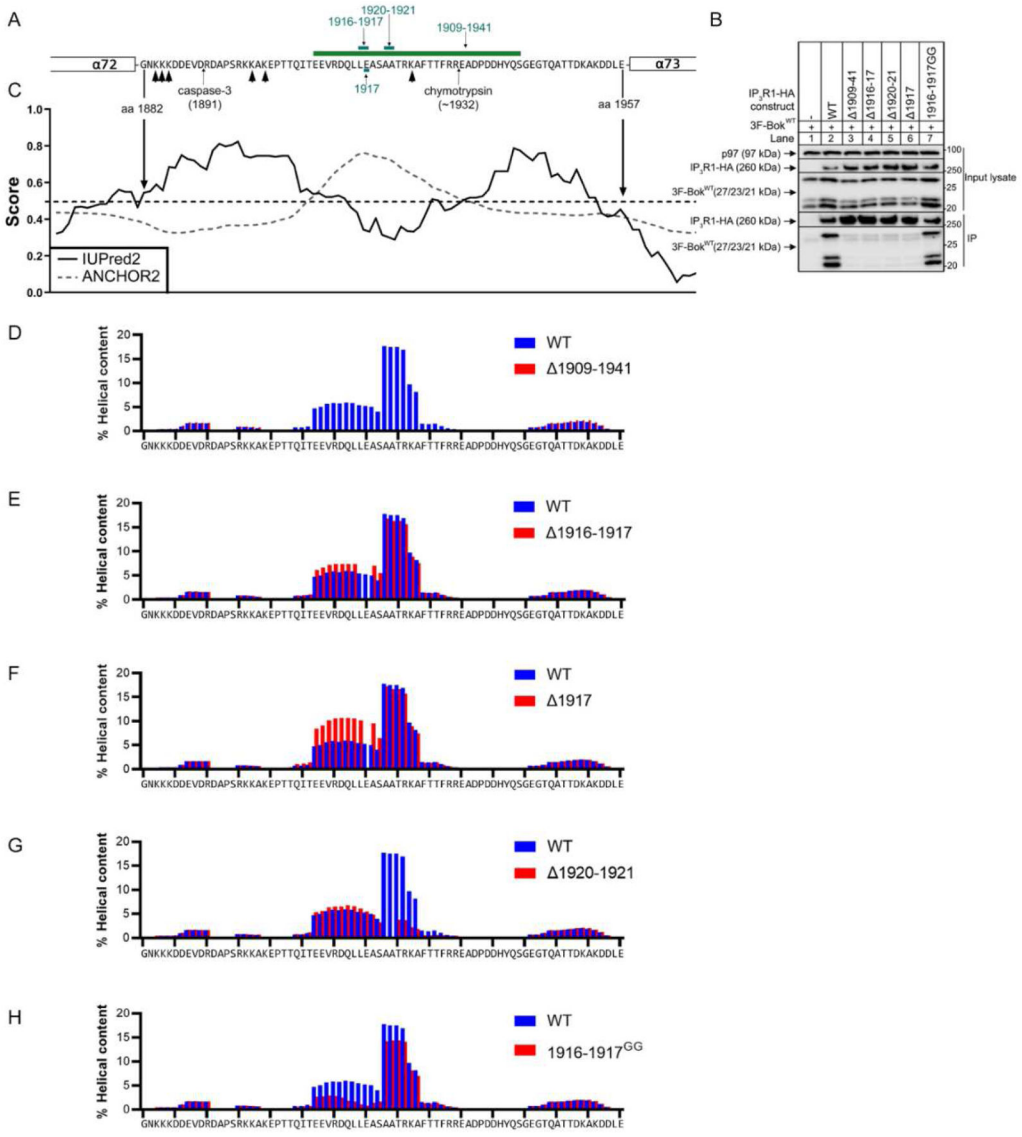

Figure 1. The Bok binding site in IP_3R1 lies within the loop between α helices 72 and 73.

A) sequence of the IP_3R1 α72-73 loop, corresponding to amino acids 1882-1957, the positions at which caspase-3 and chymotrypsin cleave IP_3R1 (arrows) [12], lysine residues known to be ubiquitinated (arrowheads) [12], and IP_3R1-HA deletion mutants (green lines). **B)** Anti-HA IP and input cell lysates from IP_3R1-HA and 3F-Bok co-transfected HEK-3KO cells probed in immunoblots for the proteins indicated; p97 serves as a loading control for the input lysates. 3F-Bok expresses as multiple anti-Bok immunoreactive species (27, 23, and 21 kDa) due to alternative translation initiation [4]. **C)** IUPred2 and ANCHOR2 scores, aligned with the sequence in A (IUPred2 long analysis, context-dependent ANCHOR2 analysis, available at https://iupred2a.elte.hu/). **D-H**) Agadir helical predictions (default settings, available at http://agadir.crg.es/). In IP_3R1 mutants, missing amino acid residues were assigned a value of 0.

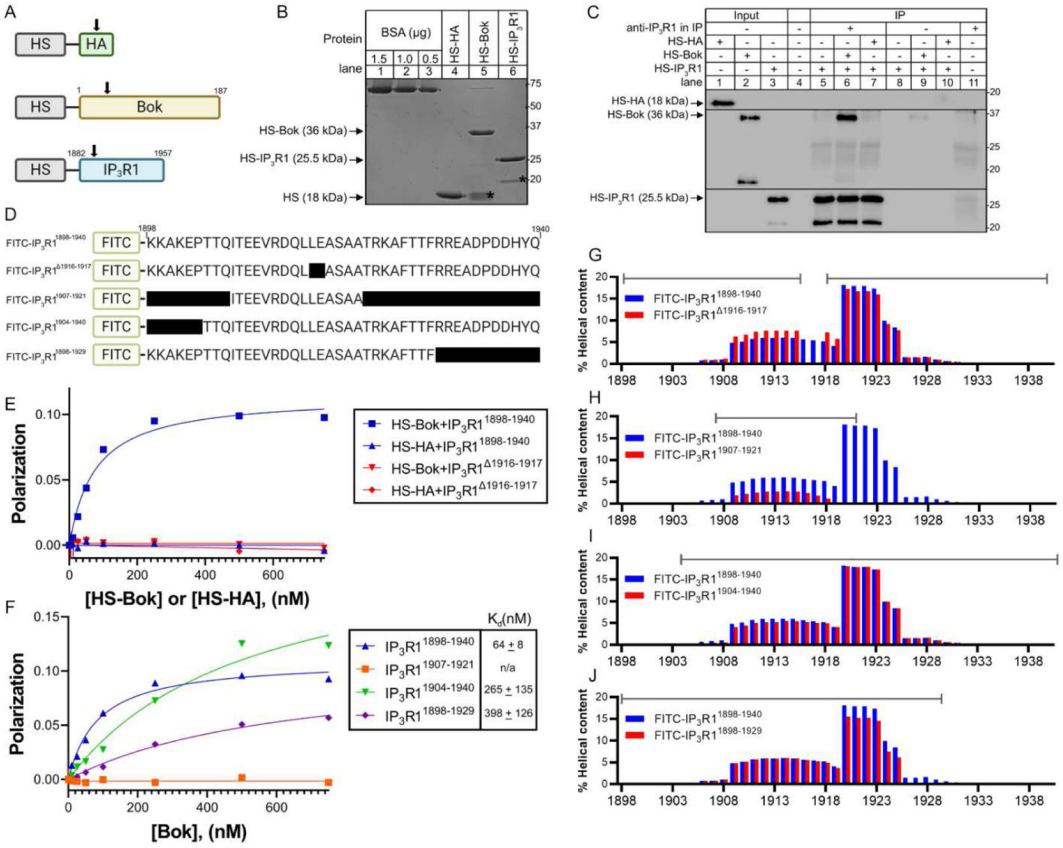

Figure 2. Bok and IP_3R1-derived peptides associate *in vitro.*

A) HS-tagged constructs expressed in bacteria. Arrowheads mark the positions of antibody epitopes used for recognition; residues 19-32 for HS-Bok, residues 1884-1903 for HS-IP_3R1, and the 9 amino acid HA tag for HS-HA. **B)** Coomassie blue-stained gel of purified bacterially-expressed HS-HA, HS-Bok and HS-IP_3R1, together with known amounts of BSA. Protein fragments (*) were present as minor contaminants in the HS-Bok and HS-IP_3R1 preparations. **C)** Purified HS-IP_3R1, HS-Bok and HS-HA were incubated as indicated in PBS / 0.1% BSA for 16h at 4°C, HS-IP_3R1 was immunoprecipitated with anti-$IP_3R1^{1884\text{-}1903}$ and immunoprecipitates (lanes 5-7), plus controls (lanes 8-11) and inputs (lanes 1-3) were probed in immunoblots for the proteins indicated. **D)** FITC-conjugated, IP_3R1-derived peptides. **E)** FP with HS-Bok or HS-HA and FITC-conjugated peptides. **F)** FP with HS-Bok and FITC-conjugated peptides, with K_d values (n=3). **G-J,** Agadir helical prediction for FITC-IP_3R1 peptides. The grey lines show the sequence encompassed in each peptide. (A. and D. created with BioRender).

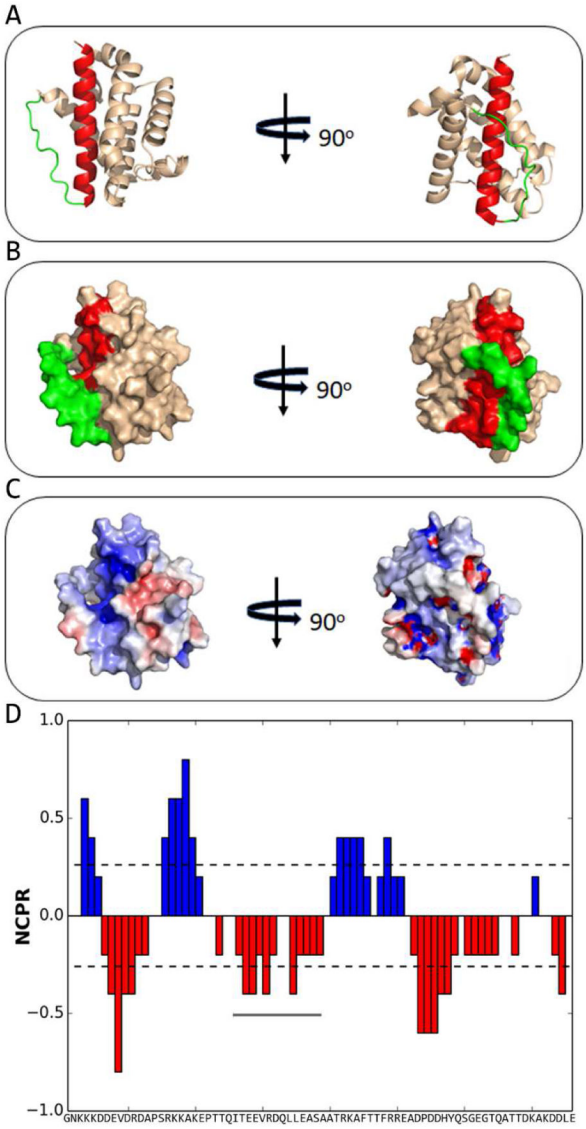

Figure 3. Structural basis of the IP_3R1 α72-73 loop interaction with Bok.

A) Cartoon, **B)** surface and **C)** electrostatic distribution in the structure of Bok (6CKV [18]) in two orientations, visualized using PyMOL. The BH4 helix (red) is not fully accessible due to the loop (green) connecting it to the next helix (A and B) and the exposed surface around the binding interface is highly positively charged (C). **D)** Net charge per residue (NCPR) of the α72-73 loop calculated using CIDER [19] (default settings, available at http://pappulab.wustl.edu/CIDER/), revealing a negative region marked with a grey line that approximates to the central region of the loop critical for Bok binding.

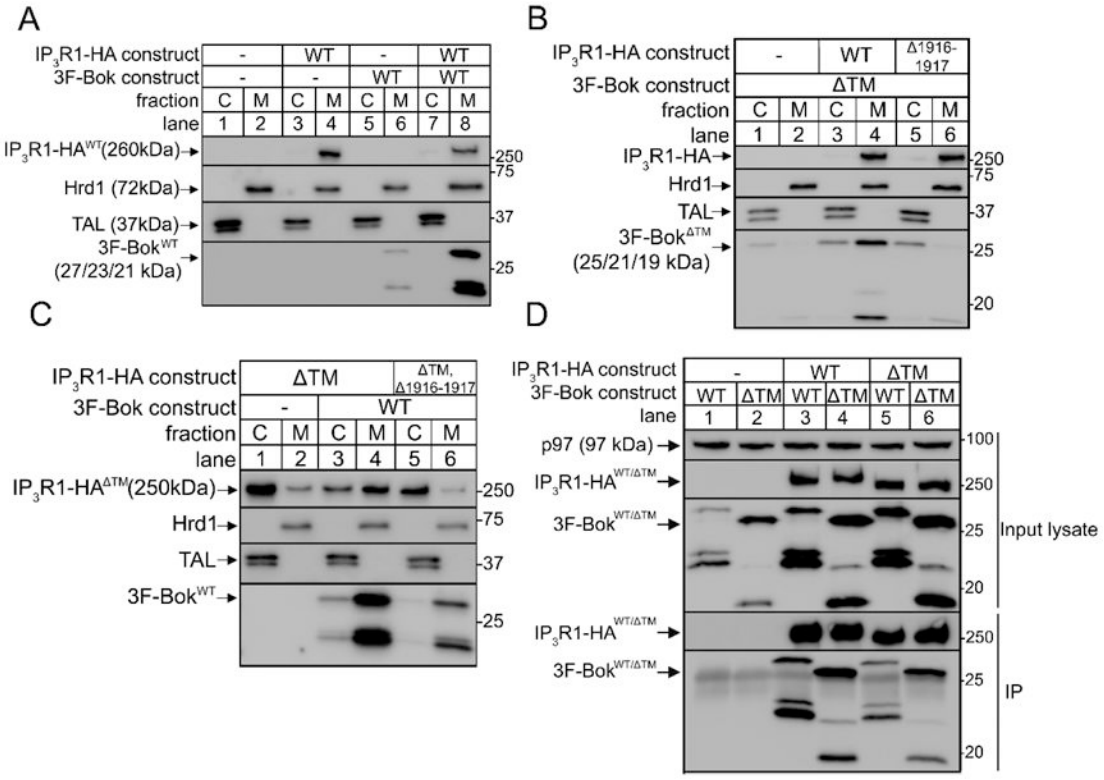

Figure 4. Bok and IP$_3$Rs associate independently of membrane insertion.

A-C) Transfected HEK-3KO cells were separated into cytosolic (C) and membrane (M) fractions and probed in immunoblots for the proteins indicated. Transaldolase (TAL) and Hrd1 serve as markers for cytosol and membrane fractions, respectively [10]. **D)** Anti-HA IP and input cell lysates from transfected HEK-3KO cells; p97 serves as a loading control for the input lysates. The constructs migrated as follows: 3F-Bok^{WT} at 27/23/21 kDa, 3F-Bok$^{\Delta TM}$ at 25/21/19 kDa, IP$_3$R1-HA^{WT} and IP$_3$R1-HA$^{\Delta 1916\text{-}1917}$ at 260kDa, and IP$_3$R1-HA$^{\Delta TM}$ and IP$_3$R1-HA$^{\Delta TM,\ \Delta 1916\text{-}1917}$ at 250kDa.